

Federated Learning of Binary Neural Networks: Enabling Low-Cost Inference

Nitin Priyadarshini Shankar*
*Department of Electrical Engineering,
 Indian Institute of Technology Madras*

ee20d425@smail.iitm.ac.in

Soham Lahiri*
*Department of Computer Science and Engineering,
 Jadavpur University*

sohaml.cse.ug@jadavpuruniversity.in

Sheetal Kalyani
*Department of Electrical Engineering,
 Indian Institute of Technology Madras*

skalyani@ee.iitm.ac.in

Saurav Prakash
*Department of Electrical Engineering,
 Indian Institute of Technology Madras*

saurav@ee.iitm.ac.in

Abstract

Federated Learning (FL) preserves privacy by distributing training across devices. However, using DNNs is computationally intensive at the low-powered edge during inference. Edge deployment demands models that simultaneously optimize memory footprint and computational efficiency, a dilemma where conventional DNNs fail by exceeding resource limits. Traditional post-training binarization reduces model size but suffers from severe accuracy loss due to quantization errors. To address these challenges, we propose FedBNN, a rotation-aware binary neural network framework that learns binary representations directly during local training. By encoding each weight as a single bit $\{+1, -1\}$ instead of a 32-bit float, FedBNN shrinks the model footprint, significantly reducing runtime (during inference) FLOPs and memory requirements in comparison to federated methods using real models. Evaluations across multiple benchmark datasets demonstrate that FedBNN significantly reduces resource consumption while performing similarly to existing federated methods using real-valued models.

1 Introduction

Federated Learning (FL) has emerged as a powerful paradigm for privacy-preserving collaborative training across distributed edge devices. In standard FL, clients locally update a shared global model using private data, while a central server aggregates these updates over multiple communication rounds. Although this framework addresses data privacy during training, it does not resolve a critical deployment challenge: modern deep neural networks remain computationally and memory-intensive at inference time. For vision applications running on resource-constrained edge devices, the runtime cost of model inference measured in memory footprint, arithmetic operations, and energy consumption often becomes the primary bottleneck. Consequently, designing models that are inherently efficient at inference is essential for enabling practical federated vision systems.

Several works focus on mitigating the communication overhead in federated learning. FedMUD Li et al. (2025) enhances the efficiency of low-rank FL by addressing three critical challenges in decomposition

*Equal contribution.

by proposing Model Update Decomposition (MUD), Block-wise Kronecker Decomposition (BKD), and Aggregation-Aware Decomposition (AAD), which are complementary and can be jointly applied. Their approach demonstrates faster convergence with improved accuracy compared to prior low-rank baselines. The authors of Kim et al. (2024a) address unstable convergence under client heterogeneity and low participation by introducing a lookahead gradient strategy. Their method broadcasts projected global updates without incurring extra communication costs or memory dependence, while additionally regularizing local updates to align with the overshoot global model. This yields improved stability and tighter theoretical convergence guarantees, particularly under partial client participation. The work in Hu et al. (2024) proposes a hybrid gradient compression (HGC) framework that reduces uplink and downlink costs by exploiting multiple forms of redundancy during training. With compression-ratio correction and dynamic momentum correction, HGC achieves a high compression ratio with negligible accuracy loss in practice.

The work in Guo & Yang (2024) addresses generalisation under client imbalance by leveraging Federated Group DRO algorithms to balance robustness and communication efficiency. FedLPA Liu et al. (2024) proposes a one-shot aggregation framework that infers layer-wise Laplace posteriors to mitigate non-IID effects without requiring auxiliary data, markedly improving one-round training performance. The work in Crawshaw & Liu (2024) studies more realistic client participation patterns and proposes Amplified SCAFFOLD, which achieves linear speedup and significantly fewer communication rounds via projected lookahead. FedSMU Lu et al. (2025) simplifies communication by symbolizing updates (i.e., transmitting signs only) while decoupling the Lion optimizer between local and global steps, tackling communication and heterogeneity. FedBAT Li et al. (2024) proposes binarization-aware training, which directly learns binary model updates during local training through a stochastic, learnable operator $S(x, \alpha)$ with trainable step size α . However, local optimization still relies on real-valued parameters, with binarization applied only to the communicated updates. Also, the final model learnt after training is real and complex.

While communication efficiency is critical in federated learning (FL), maintaining lightweight models after training is equally important for resource-constrained edge devices. SpaFL Kim et al. (2024b) introduces trainable per-filter thresholds to induce structured sparsity, requiring only threshold vectors to be uploaded, which leads to improved accuracy and reduced communication cost relative to sparse baselines. In contrast, our client-side Binary Neural Networks (BNNs) employ binary filters ($\{-1, +1\}$), reducing runtime computation and memory usage. BiPruneFL Lee & Jang (2025) combines binary quantization with pruning to lower computation and communication costs, achieving up to two orders of magnitude efficiency gains while retaining accuracy comparable to uncompressed models. Similarly, the work in Shah & Lau (2023) explores sparsification and quantization to address uplink and downlink communication, demonstrating superior trade-offs between model compression and accuracy preservation. The authors of Yang et al. (2021) specifically study BNNs in FL, where clients transmit only binary parameters, and a Maximum Likelihood (ML) based reconstruction scheme is used to recover real-valued global parameters. Their framework effectively reduces communication costs while establishing theoretical convergence conditions for training federated BNNs.

In this work, we address the challenge of reducing runtime computational complexity in FL models on edge devices while maintaining high performance. Building on the idea of rotated binary neural networks Lin et al. (2020), we introduce FedBNN, a federated learning strategy inspired by FedAvg, which trains a rotated binary neural network with binary weights while preserving the same parameter count as its real-valued counterpart. Despite this parity, the binary representation of the global model yields substantial gains in memory efficiency and runtime computational savings. Our main contributions are as follows:

1. We propose FedBNN, an FL framework for training Binary Neural Networks (BNNs) that achieve lower runtime computation and memory complexity than real-valued models.
2. We conduct a comprehensive comparison of FedBNN against state-of-the-art federated learning methods: FedAvg, FedBAT, and FedMUD, across diverse benchmark datasets such as FMNIST, SVHN, CIFAR-10, TinyImageNet, and FEMNIST. Additionally, we evaluate performance under three different data heterogeneity settings to ensure a robust assessment.
3. We analyze the runtime complexity of FedBNN in terms of computational cost and memory consumption, highlighting its efficiency advantages over existing approaches.

-
4. We evaluate the post-training binarization performance of FedBNN against state-of-the-art methods, demonstrating its effectiveness and superior efficiency in resource-constrained environments.

2 Preliminaries

2.1 Federated Learning

Federated Learning is a distributed machine learning paradigm that enables multiple clients to collaboratively train a shared model while keeping their data decentralized. Unlike traditional centralized learning, FL addresses critical challenges including data privacy, communication constraints, and statistical heterogeneity across participants. The authors of McMahan et al. (2017) introduced the Federated Averaging (FedAvg) algorithm, which combines local stochastic gradient descent on individual clients with periodic model averaging on a central server. The method addresses the fundamental optimization problem:

$$\min_{\mathbf{w} \in \mathbb{R}^d} \mathcal{L}(\mathbf{w}) \quad \text{where} \quad \mathcal{L}(\mathbf{w}) = \frac{1}{N_s} \sum_{i=1}^{N_s} \mathcal{L}_i(\mathbf{w}) \quad (1)$$

Here, \mathcal{L}_i is the loss for a particular sample (x_i, y_i) , \mathbf{w} is the model parameter, N_s is the total number of samples. In the federated setting with N_k clients, this is reformulated as:

$$\mathcal{L}(\mathbf{w}) = \sum_{k=1}^{N_k} \frac{N_{sk}}{N_s} l_k(\mathbf{w}) \quad \text{where,} \quad l_k(\mathbf{w}) = \frac{1}{N_{sk}} \sum_{i \in \mathcal{P}_k} \mathcal{L}_i(\mathbf{w}) \quad (2)$$

Here, \mathcal{P}_k represents the data partition on client k and $N_{sk} = |\mathcal{P}_k|$. The FedAvg algorithm operates by selecting a fraction N_{cr} of clients each round, having each perform N_e local epochs of SGD with batch size N_b : $\mathbf{w} \leftarrow \mathbf{w} - \eta \nabla \mathcal{L}(\mathbf{w}; b)$ for each batch b , followed by server-side weighted averaging:

$$\mathbf{w}_{t+1} \leftarrow \sum_{k=1}^{N_k} \frac{N_{sk}}{N_s} \mathbf{w}_{t+1}^k \quad (3)$$

2.2 Binarized Neural Network

If $g_\phi(\cdot)$ is a CNN with L layers, its parameters are given by $\phi = \{\mathbf{W}_1, \dots, \mathbf{W}_L\}$, where $\mathbf{W}_l \in \mathbb{R}^{c_o \times c_i \times k \times k}$ represents the weight matrix of the l^{th} layer. Here, c_i and c_o represent the input and output channels, respectively, and k denotes the filter size. In a Binary Neural Network (BNN), both weights (\mathbf{W}_l) and activations (\mathbf{a}_l) are binarized using the sign function:

$$\mathbf{W}_l^b = \text{sign}(\mathbf{W}_l), \quad \mathbf{a}_l^b = \text{sign}(\mathbf{a}_l), \quad (4)$$

and the convolution is approximated using bit-wise operations:

$$\mathbf{W}_l * \mathbf{a}_l \approx \mathbf{W}_l^b \circledast \mathbf{a}_l^b, \quad (5)$$

where \circledast denotes bit-wise convolution (like XNOR and bit count). Although the forward pass uses binarized values, real-valued weights and gradients are retained for backpropagation. Due to the non-differentiability of the sign function, whose derivative is zero almost everywhere, training binarized neural networks poses significant challenges, particularly in backpropagation, where meaningful gradients are required. Hence, a straight-through estimator (STE) is used: if $b = \text{sign}(r)$, then:

$$\nabla_r = \nabla_b \cdot \mathbf{1}_{|r| \leq 1}, \quad (6)$$

where $\nabla_r = \frac{\partial C}{\partial r}$, $\nabla_b = \frac{\partial C}{\partial b}$, and C is the cost function. To ensure stable updates, real weights are clipped to the range $[-1, 1]$. We adopt the approach from Hubara et al. (2016) to implement binarized convolution

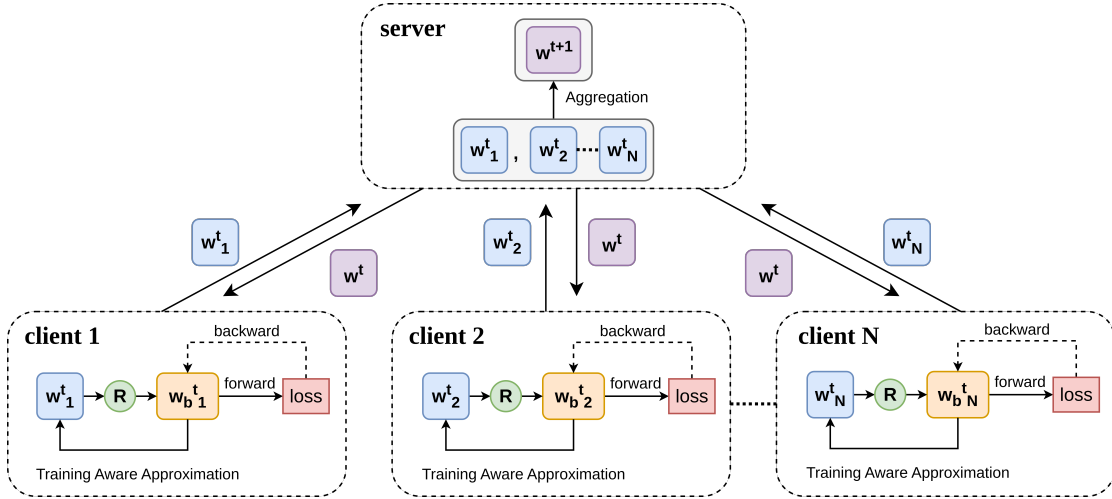


Figure 1: FedBNN overall architecture.

layers, converting floating-point operations into efficient XNOR and bit-count operations. While this drastically reduces computation and memory usage, it often comes at the cost of reduced accuracy. One key limitation of BNNs is the quantization error caused by binarizing the weight vector $\mathbf{w}_l \in \mathbb{R}^{n_l}$, which is the flattened form of \mathbf{W}_l , where $n_l = c_o \cdot c_i \cdot k^2$. This error arises due to the angular bias (ϕ) between \mathbf{w}_l and its binarized version \mathbf{w}_l^b , potentially degrading network performance.

3 Proposed Method - FedBNN

3.1 Proposed Rotation-Aware Client Training

3.1.1 Trainable rotation weight with global memory

To address the angular bias, the authors of Lin et al. (2020) proposed applying a rotation matrix $\mathbf{R}_l \in \mathbb{R}^{n_l \times n_l}$ at the start of each training epoch to minimize the angle ϕ_l between $(\mathbf{R}_l)^T \mathbf{w}_l$ and $\text{sign}((\mathbf{R}_l)^T \mathbf{w}_l)$. Building on this, we propose the use of a fused weight \mathbf{w} that interpolates between the client and server weight representations as shown below:

$$\mathbf{w} = \lambda_l \mathbf{w}_l + (1 - \lambda_l) \mathbf{w}_{\text{server}} \quad (7)$$

Here, $\lambda_l = \text{sigmoid}(\omega_l) \in [0, 1]$, ω_l is a trainable parameter, and $\mathbf{w}_{\text{server}}$ is the aggregated weight sent from the server as shown in Eq. (3). During the first local epoch of each client, the local weights are initialized from the global model, and the fused representation effectively reduces to $\mathbf{w}_{\text{server}}$. In subsequent local epochs, \mathbf{w} becomes a convex combination of the evolving client weights \mathbf{w}_l and the server weights $\mathbf{w}_{\text{server}}$. The rotation is then applied to this fused vector \mathbf{w} , aligning the quantization process with a federated-aware representation while jointly capturing both local and global model information. This rotation is applied to the weights of each layer in every epoch of every round, as shown in Figure 1. Below, we discuss the entire rotation process. For simplicity, we omit subscripts denoting the layer, client, or epoch in the following discussion. To minimize the angular bias (ϕ), $\cos(\phi)$ needs to be maximized and hence, the optimization is formulated as follows:

$$\cos(\phi) = \frac{\text{sign}((\mathbf{R})^T \mathbf{w})^T ((\mathbf{R})^T \mathbf{w})}{\|\text{sign}((\mathbf{R})^T \mathbf{w})\|_2 \|((\mathbf{R})^T \mathbf{w})\|_2}, \quad (8)$$

where $(\mathbf{R})^T \mathbf{R} = \mathbf{I}_n$ is the n -th order identity matrix. Note, $\|\text{sign}((\mathbf{R})^T \mathbf{w})\|_2 = \sqrt{n}$ and $\|((\mathbf{R})^T \mathbf{w})\|_2 = \|\mathbf{w}\|_2$. Since the training happens at the beginning of each epoch, we can take $\|\mathbf{w}\|_2$ to be a constant. With

Algorithm 1: Federated Binary Neural Network (FedBNN) training. The N_k clients are indexed by k ; N_b is the local minibatch size, N_e is the number of local epochs, and η is the learning rate. N_{cr} is the number of clients selected per round. N_{eR} is the number of epochs of rotation. N_{lR} is the number of layers that require rotation. Θ is the set of all trainable parameters.

Server executes:

initialize \mathbf{w}_0

for *round* **in** $\text{range}(N_r)$ **do**

$S_t \leftarrow$ (random set of N_{cr} clients)

for *each client* $\in S_t$ **in parallel** **do**

$\mathbf{w}_{t+1}^k \leftarrow$ **ClientUpdate** (k, \mathbf{w}_t)

end

$\mathbf{w}_{t+1} = \sum_{k=1}^K \frac{N_{sk}}{N_k} \mathbf{w}_{t+1}^k$

end

ClientUpdate ($k, \mathbf{w}_{\text{server}}$):

$\mathcal{B} \leftarrow$ (split \mathcal{P}_k into batches of size N_b)

$\mathbf{w} \leftarrow \mathbf{w}_{\text{server}}$

for *epoch* **in** $\text{range}(N_e)$ **do**

for e_R **in** $\text{range}(N_{eR})$ **do**

for l **in** $\text{range}(N_{lR})$ **do**

$\mathbf{W}'_l \leftarrow \text{sign}((\mathbf{R}_{l1})^T \overline{\mathbf{W}}_l \mathbf{R}_{l2})$

$\mathbf{U}_1, \mathbf{S}_1, \mathbf{V}_1 \leftarrow \text{SVD}(\mathbf{W}'_l (\mathbf{R}_{l2})^T (\overline{\mathbf{W}}_l)^T)$

$\mathbf{R}_{l1} \leftarrow \mathbf{V}_1 (\mathbf{U}_1)^T$

$\mathbf{U}_2, \mathbf{S}_2, \mathbf{V}_2 \leftarrow \text{SVD}((\overline{\mathbf{W}}_l)^T \mathbf{R}_{l1} \mathbf{W}'_l)$

$\mathbf{R}_{l2} \leftarrow \mathbf{U}_2 (\mathbf{V}_2)^T$

end

end

for *batch* $b \in \mathcal{B}$ **do**

for $\theta \in \Theta$ **do**

$\theta \leftarrow \theta - \eta \sigma_\theta(b)$

end

end

end

return \mathbf{w} to server

the help of algebraic manipulations, we get $\mathbf{W}'^b = \text{sign}((\mathbf{R}_1)^T \overline{\mathbf{W}} \mathbf{R}_2)$, $\text{Vec}(\overline{\mathbf{W}}) = \mathbf{w}$, $\overline{\mathbf{W}} \in \mathbb{R}^{n_1 \times n_2}$ and

$$\mathbf{w}^T \mathbf{R} = \mathbf{w}^T (\mathbf{R}_1 \otimes \mathbf{R}_2) = \text{Vec}((\mathbf{R}_2)^T (\overline{\mathbf{W}})^T \mathbf{R}_1) \quad (9)$$

where \otimes is the Kronecker product and the operation $\text{Vec}(\cdot)$ vectorizes an input matrix. The final optimization objective is given by

$$\begin{aligned} & \arg \max_{\mathbf{W}'^b, \mathbf{R}_1, \mathbf{R}_2} \text{tr}(\mathbf{W}'^b (\mathbf{R}_2)^T (\overline{\mathbf{W}})^T \mathbf{R}_1) \\ & \text{s.t. } \mathbf{W}'^b \in \{+1, -1\}^{n_1 \times n_2} \\ & \quad (\mathbf{R}_1)^T \mathbf{R}_1 = \mathbf{I}_{n_1} \\ & \quad (\mathbf{R}_2)^T \mathbf{R}_2 = \mathbf{I}_{n_2}. \end{aligned} \quad (10)$$

Since the above optimization is a non-convex problem, an alternating optimization approach is used, where one variable is updated, keeping the other two fixed until convergence. We, therefore, have three optimization steps, as shown in Algorithm 1:

1. The first step is to learn \mathbf{W}'^b while fixing \mathbf{R}_1 and \mathbf{R}_2 . It is solved by

$$\mathbf{W}'^b = \text{sign}((\mathbf{R}_1)^T \overline{\mathbf{W}} \mathbf{R}_2) \quad (11)$$

2. The next step updates \mathbf{R}_1 while keeping \mathbf{W}'^b and \mathbf{R}_2 constant. Performing $\text{SVD}(\mathbf{W}'^b (\mathbf{R}_2)^T (\overline{\mathbf{W}})^T) = \mathbf{U}_1 \mathbf{S}_1 (\mathbf{V}_1)^T$, it is solved by

$$\mathbf{R}_1 = \mathbf{V}_1 (\mathbf{U}_1)^T. \quad (12)$$

3. Similar to the previous steps, the following step updates \mathbf{R}_2 while keeping \mathbf{W}'^b and \mathbf{R}_1 constant. Performing $\text{SVD}((\overline{\mathbf{W}})^T \mathbf{R}_1 \mathbf{W}'^b) = \mathbf{U}_2 \mathbf{S}_2 (\mathbf{V}_2)^T$, it is solved by

$$\mathbf{R}_2 = \mathbf{U}_2 (\mathbf{V}_2)^T \quad (13)$$

3.1.2 Adjustable rotated weight vector for federated learning with global memory

The optimization steps described above are executed iteratively. The variables \mathbf{W}'^b , \mathbf{R}_1 , and \mathbf{R}_2 typically converge within three iterations. However, the process may still get trapped in a local optimum due to overshooting/undershooting. An adjustable rotated weight vector scheme was used to further reduce angular bias after the bi-rotation step. However, in a federated setting, a client may need to align its weights not just with its own rotated representation but also with $\mathbf{w}_{\text{server}}$. To this end, we propose a generalized update:

$$\tilde{\mathbf{w}} = \mathbf{w} + \alpha\beta(\mathbf{R}^T \mathbf{w} - \mathbf{w}) + \alpha(1 - \beta)(\mathbf{w}_{\text{server}} - \mathbf{w}) \quad (14)$$

where \mathbf{w} is the interpolated weight, $\alpha = |\sin(\theta)|$, $\beta = |\sin(\gamma)|$, $\theta, \gamma \in \mathbb{R}$ are learnable parameters controlling the contributions from the rotated and server weights. Our proposed parameterisation using $\alpha\beta$ and $\alpha(1 - \beta)$ ensures that the resulting coefficient of \mathbf{w} in Eq. equation 14 remains non-negative, thereby preserving update stability while enabling a convex combination of the rotated and server-aligned directions. The added regularization term $(\alpha(1 - \beta)(\mathbf{w}_{\text{server}} - \mathbf{w}))$ updates adaptively and fuses local and global knowledge while correcting angular bias with respect to both. It gathers inspiration from Li et al. (2020), where a proximal term is added to prevent training divergence due to heterogeneous data. While the original method in Lin et al. (2020) is designed for centralized training, we extend this framework to federated learning.

In summary, each client receives the global server weight $\mathbf{w}_{\text{server}}$ at the beginning of each round. We introduce a learnable fusion parameter λ_l to interpolate between the client and server weights, forming a federated-aware fused weight \mathbf{w} . The bi-rotation is then applied to \mathbf{w} instead of \mathbf{w}_l , allowing angular correction in the shared representation space. Moreover, we introduce two additional learnable scalars α_l and β_l to adaptively adjust the influence of the rotated direction and the global server model, respectively, during the binarization step.

3.1.3 Training aware approximation for federated learning

To improve upon the STE, the work in Lin et al. (2020) introduced a training-aware approximation function that serves as a smooth, epoch-dependent surrogate for the sign function, enabling better gradient flow during early training. Unlike centralized training, where t and k are updated each epoch locally, our federated setup maintains these values across global rounds to ensure consistent client training behavior. The approximation is given by:

$$F(x) = \begin{cases} k \cdot \left(-\text{sign}(x) \cdot \frac{t^2 x^2}{2} + \sqrt{2} t x \right), & \text{if } |x| < \frac{\sqrt{2}}{t}, \\ k \cdot \text{sign}(x), & \text{otherwise,} \end{cases} \quad (15)$$

where the coefficients t and k evolve with training as:

$$t = 10^{(T_{\min}) + \frac{(rN_e + e)}{N_r N_e} (T_{\max} - T_{\min})} \quad (16)$$

$$k = \max\left(\frac{1}{t}, 1\right) \quad (17)$$

where $T_{\min} = -2$, $T_{\max} = 1$, N_r the total number of global training rounds, and r the current round index, N_e the total number of local training epochs, and e the current epoch of training. The derivative of this function with respect to x is:

$$F'(x) = \frac{\partial F(x)}{\partial x} = \max\left(k \cdot (\sqrt{2}t - |t^2x|), 0\right), \quad (18)$$

which yields non-zero gradients during early training, allowing effective optimization of both client and server-side parameters, and progressively transitions to a sign-like function, thus preserving binarization.

Using this surrogate, we compute gradients of the loss \mathcal{L} with respect to both activations \mathbf{a} and the mixed weights $\tilde{\mathbf{w}}$ as follows:

$$\sigma_{\mathbf{a}} = \frac{\partial \mathcal{L}}{\partial F(\mathbf{a})} \cdot \frac{\partial F(\mathbf{a})}{\mathbf{a}}, \quad (19)$$

$$\sigma_{\mathbf{w}} = \frac{\partial \mathcal{L}}{\partial F(\tilde{\mathbf{w}})} \cdot \frac{\partial F(\tilde{\mathbf{w}})}{\partial \tilde{\mathbf{w}}} \cdot \frac{\partial \tilde{\mathbf{w}}}{\partial \mathbf{w}}, \quad (20)$$

where the mixed-weight Jacobian is defined as:

$$\frac{\partial \tilde{\mathbf{w}}}{\partial \mathbf{w}} = (1 - \alpha) \cdot \mathbf{I}_n + \alpha \beta \cdot \mathbf{R}^\top, \quad (21)$$

accounting for both the direct client path and the rotation-aligned correction. The gradients of the adaptive mixing parameters α and β , which respectively control the contributions from the rotation-aligned direction and the global server model, are computed as:

$$\sigma_{\alpha} = \frac{\partial \mathcal{L}}{\partial \tilde{\mathbf{w}}} \cdot \{\beta(\mathbf{R}^\top \mathbf{w} - \mathbf{w}_{\text{server}}) + (\mathbf{w}_{\text{server}} - \mathbf{w})\} \quad (22)$$

$$\sigma_{\beta} = \frac{\partial \mathcal{L}}{\partial \tilde{\mathbf{w}}} \cdot \{\alpha(\mathbf{R}^\top \mathbf{w} - \mathbf{w}_{\text{server}})\} \quad (23)$$

This training-aware formulation plays a critical role in stabilizing federated optimization by aligning binarization with geometric orientation and enabling meaningful gradient flow throughout local client training, as shown in Figure 1. In summary, at the beginning of every training epoch of each client, the rotation matrices, \mathbf{R}_1 and \mathbf{R}_2 , are learned for a fixed \mathbf{w} . At the training phase, with the fixed \mathbf{R}_1 and \mathbf{R}_2 , the proposed model takes the sign of parameter $\tilde{\mathbf{w}}$ for the forward pass and the parameters \mathbf{w}_l , α and β are updated during back-propagation, which enables the network to learn a suitable value that further optimizes the application of the rotation in equation (16).

Choice of λ , α , and β : In the proposed method, λ , α , and β are treated as trainable parameters rather than hyperparameters, enabling the network to automatically learn optimal values for each layer. The variation of these parameters across training rounds for different layers is illustrated in the supplementary.

3.2 Proposed Aggregation Strategy

In FedBNN, the server maintains two parallel representations of the global model: (i) an aggregated *real-valued* weight vector that is communicated to clients, and (ii) an aggregated *rotation-aligned* weight vector that is used exclusively for model evaluation and selection. After local training, each client transmits its updated real-valued weights \mathbf{w}_k together with the corresponding learned rotation matrices \mathbf{R}_k to the server. The increase in the number of bits transmitted to the server, introduced by \mathbf{R}_1 and \mathbf{R}_2 , is less than 1% for CNN4, and it becomes increasingly negligible as model size increases (details are provided in the supplementary). At the server, two separate aggregations are performed. First, the real-valued weights are aggregated in the standard FedAvg manner to produce the global model, which is then broadcast to clients

according to Eq. (4) ($\mathbf{w}_{\text{server}}$ is the same as \mathbf{w}_t). Second, for the purpose of binarization-aware evaluation, the server computes rotation-aligned weights for each client and aggregates them in the rotated space:

$$\mathbf{w}_{R,t+1} = \sum_{k=1}^{N_k} \frac{N_{sk}}{N_s} (\mathbf{R}_k^\top \mathbf{w}_k). \quad (24)$$

These two aggregated quantities are combined only at the server side through a modified update rule derived from Eq. (14). Specifically, the server forms an auxiliary update

$$\tilde{\mathbf{w}} = \mathbf{w}_{t+1} + \alpha\beta (\mathbf{w}_{R,t+1} - \mathbf{w}_{t+1}) + \alpha(1 - \beta) (\mathbf{w}_t - \mathbf{w}_{t+1}), \quad (25)$$

where \mathbf{w}_t denotes the server model from the previous communication round. Importantly, $\tilde{\mathbf{w}}_{t+1}$ is *not* transmitted to clients; it is used solely to evaluate performance and to identify the best global model during training. The model broadcast to clients in the next round is always the aggregated real-valued model \mathbf{w}_{t+1} . Upon reception, each client initializes its local parameters with \mathbf{w}_{t+1} and continues local optimization while jointly updating both the real-valued weights and the rotation matrices.

Using rotation-aligned aggregation only for server-side evaluation provides a reliable, binarization-aware criterion for model selection. Because the learned rotations explicitly reduce the angular mismatch between real-valued weights and their binarized counterparts, averaging in the rotated space preserves sign consistency across clients and mitigates quantization noise. As a result, the selected global model lies closer to a binarization-friendly manifold, leading to improved stability of the sign operation and higher binary accuracy, without altering the communication protocol or client-side optimization.

3.3 Runtime computation savings for binary models

From Shankar et al. (2024), we estimate the number of runtime multiplication and addition operations in a 2D CNN for comparison. For a convolution between real-valued $\mathbf{W}_l \in \mathbb{R}^{c_o \times c_i \times k \times k}$ and input $\mathbf{a}_l \in \mathbb{R}^{c_i \times h_{in}^w \times h_{in}^h}$, the output is $\mathbf{a}_{l+1} \in \mathbb{R}^{c_o \times h_{out}^w \times h_{out}^h}$. The number of multiplications is $c_i \cdot k^2 \cdot h_{out}^w \cdot h_{out}^h \cdot c_o$, and additions are roughly of the same order. Thus, the total FLOPs for the l^{th} layer is approximately $2 \cdot c_i \cdot k^2 \cdot h_{out}^w \cdot h_{out}^h \cdot c_o$. Also, we consider every parameter to be of 32 bits. Hence, to calculate the total memory, we multiply the total parameters by 32. By binarizing weights and activations to $\{+1, -1\}$, convolutions are replaced by efficient XNOR and bit-count operations. And all the weights will only need 1 bit for storage. The work in Rastegari et al. (2016) states that using binary neural networks results in a FLOPs reduction of $58\times$ and memory savings of $32\times$. Hence, to compare FedBNN with real models, we use this conversion factor to estimate the computational savings in FLOPs and memory.

4 Experimental Evaluation

4.1 Setup

All experiments are implemented using the PyTorch framework and executed on a server with two NVIDIA RTX PRO 6000 GPUs. We conduct federated training with $N_c = 100$ clients per experiment. The training follows the standard federated averaging (FedAvg) protocol for model synchronization. We use stochastic gradient descent with a learning rate of 0.1 for CNN4, ResNet10, and ResNet18, and 0.01 for ConvNeXt-Tiny for optimization. The learning rate is decreased by a factor of 2 at uniformly spaced intervals throughout the total training rounds, starting at round 200. 10 clients are randomly sampled for local model updates in each round. Each federated training round consists of 15 local epochs (5 for FMNIST and 10 for SVHN), with a mini-batch size of 64. The global training process runs for 1500 rounds (500 for FMNIST and SVHN) in total.

4.2 Datasets and Partitioning

To comprehensively evaluate the effectiveness of FedBNN, we conduct experiments on several widely used federated learning benchmarks, namely, FMNIST, SVHN, CIFAR10, Tiny-ImageNet, and FEMNIST. The

client models are trained on the partitioned training data for all experiments. The testing data is split into two equal sets: validation and testing. The best model is picked at the server after aggregation based on the validation set. The final performance of the model is reported on the unseen test set. To thoroughly assess our approach’s performance on data heterogeneity, we evaluate under both IID and non-IID data distribution scenarios, following federated learning benchmarks McMahan et al. (2017). Under IID partitioning, each client is assigned an equal share of randomly sampled data, resulting in locally similar datasets. The non-IID setting comprises two configurations: Non-IID 1 and Non-IID 2. In Non-IID 1, samples are distributed among clients according to a Dirichlet distribution Hsu et al. (2019), with the Dirichlet parameter α modulating the degree of statistical skew, set to 0.3 for all the datasets. Non-IID 2 represents an extreme heterogeneity case, where each client receives data from only a subset of possible labels, specifically, 10 random labels per client for CIFAR-100 and 3 random labels per client for the other datasets. These partitioning strategies enable a systematic examination of model performance as data distributions on clients become increasingly disparate, closely mirroring realistic federated deployment scenarios.

4.3 Simulation results

4.3.1 Performance comparison across datasets and methods

Table 1 presents a comprehensive comparison of FedBNN, FedAvg, FedBAT, and FedMUD across seven datasets and multiple model architectures under IID and Non-IID data distributions. As expected, FedAvg consistently achieves the highest clean accuracy, benefiting from full-precision training and communication. However, FedBNN remains highly competitive and often outperforms other binarization-aware baselines. On FMNIST (CNN4), FedBNN achieves 88.46%, 87.76%, and 83.38% under IID, Non-IID 1, and Non-IID 2, respectively. While this is below FedAvg (92.24%, 91.44%, 89.28%), FedBNN closely matches FedMUD (89.60%, 88.60%, 86.00%) and outperforms FedBAT under Non-IID 1 by 0.1%. On SVHN, FedBNN achieves 86.89%, 85.63%, and 84.40% respectively, outperforming FedBAT by large margins (+0.88%, +4.80%, and +8.62%) and remaining close to FedMUD, which achieves 86.31%, 84.38%, and 83.14%. Notably, FedBNN slightly surpasses FedMUD across all SVHN splits, indicating better robustness to data heterogeneity.

On CIFAR10 (ResNet10), FedBNN attains 89.95% under IID data, exceeding FedMUD (88.74%) and approaching FedAvg (90.86%). Under Non-IID settings, FedBNN achieves 82.84% and 73.82%, significantly outperforming FedBAT (72.80%, 63.70%) and remaining competitive with FedMUD (84.22%, 67.22%). We find that, with the ConvNeXt-Tiny architecture on CIFAR10, FedBNN demonstrates particularly strong performance, achieving 72.08% (IID) and 67.08% (Non-IID 1), surpassing FedAvg by +6.86% and +6.88%, and outperforming FedMUD by even larger margins. This highlights that FedBNN can outperform full-precision and mixed-precision baselines when model capacity and data heterogeneity interact unfavourably with standard aggregation methods.

On larger and more challenging datasets, FedBNN continues to exhibit strong clean accuracy. On Tiny ImageNet (ResNet18), FedBNN attains 46.54%, 43.00%, and 45.74% under IID, Non-IID 1, and Non-IID 2 settings, respectively. In this case, FedBNN significantly outperforms FedBAT across all splits while remaining within 8–9% of FedAvg, demonstrating strong performance despite the constraints of binary networks. Similarly, on FEMNIST, FedBNN achieves 79.73%, 80.31%, and 79.13% across the IID, Non-IID 1, and Non-IID 2 partitions. These results nearly match FedAvg and slightly outperform FedMUD under the Non-IID 1 setting, highlighting the robustness of FedBNN in highly heterogeneous user-level federated scenarios. Overall, these results demonstrate that FedBNN maintains strong clean accuracy across diverse datasets and data distributions, while consistently outperforming other binary federated baselines and remaining competitive with full-precision federated approaches.

4.3.2 Computation and Memory savings

Across all datasets and architectures, FedBNN consistently delivers orders-of-magnitude reductions in computational and memory cost relative to all baselines. For FMNIST and SVHN, FedBNN reduces FLOPs from 2.02×10^7 to 3.48×10^5 , achieving approximately a $58\times$ reduction, while memory usage drops from roughly 1.6 MB to 0.05 MB ($32\times$). On CIFAR10 (ResNet10), FLOPs are reduced from 4.40×10^8 to 1.11×10^7 and memory from 19.6 MB to 0.613 MB. Even for deeper architectures such as ResNet18 on Tiny-ImageNet and

Table 1: Performance comparison for $N_c = 100$. The FLOPs and memory values are calculated during runtime. Binarized accuracy refers to the model’s performance after the weights and activations have been binarized.

Method	Dataset (Model)	Accuracy			FLOPs	Memory (MB)	Binarized Accuracy		
		IID	Non - IID 1	Non - IID 2			IID	Non - IID 1	Non - IID 2
FedAvg	FMNIST (CNN4)	92.24	91.44	89.28	2.02×10^7	1.5635	53.42	63.68	54.72
FedBAT		89.12	87.66	85.56	2.02×10^7	1.5635	14.34	16.98	8.0
FedMUD		89.60	88.60	86.00	2.02×10^7	1.6291	63.2	66.5	66.08
FedBNN		88.46	87.76	83.38	3.48×10^5	0.0489	88.46	87.76	83.38
FedAvg	SVHN (CNN4)	92.10	90.60	89.34	3.00×10^7	1.5965	28.01	22.56	16.92
FedBAT		86.01	80.83	75.78	3.00×10^7	1.5965	50.35	26.69	34.71
FedMUD		86.31	84.38	83.14	3.00×10^7	1.6127	69.92	50.87	51.19
FedBNN		86.89	85.63	84.40	5.19×10^5	0.0498	86.89	85.63	84.40
FedAvg	CIFAR10 (ResNet10)	90.86	86.28	70.62	4.40×10^8	19.6170	17.2	11.38	12.74
FedBAT		89.38	72.80	63.70	4.40×10^8	19.6170	13.62	10.94	10.26
FedMUD		88.74	84.22	67.22	4.40×10^8	19.6170	15.54	10.78	18.98
FedBNN		89.95	82.84	73.82	1.11×10^7	0.6130	89.95	82.84	73.82
FedAvg	CIFAR10 (ConvNeXt-Tiny)	65.22	60.20	61.84	2.98×10^9	111.640	18.04	21.64	16.56
FedBAT		66.04	64.22	61.88	2.98×10^9	111.640	14.90	21.42	16.54
FedMUD		53.92	54.30	38.18	2.98×10^9	111.640	40.46	35.44	29.50
FedBNN		72.08	67.08	63.00	6.07×10^7	3.4887	72.08	67.08	63.00
FedAvg	Tiny-ImageNet (ResNet18)	55.00	52.62	54.54	4.44×10^9	45.090	0.52	0.52	0.56
FedBAT		27.30	32.12	20.90	4.44×10^9	45.090	0.60	0.48	0.80
FedMUD		47.20	44.16	46.06	4.44×10^9	45.090	16.24	12.80	15.60
FedBNN		46.54	43.00	45.74	9.05×10^7	1.41	46.54	43.00	45.74
FedAvg	FEMNIST (ResNet18)	80.24	81.12	80.32	9.13×10^8	45.090	2.08	1.66	1.62
FedBAT		76.44	74.31	78.41	9.13×10^8	45.090	0.38	2.08	2.40
FedMUD		78.79	80.11	76.68	9.13×10^8	45.090	25.74	0.76	0.80
FedBNN		79.73	80.31	79.13	1.84×10^7	1.41	79.73	80.31	79.13

FEMNIST, FedBNN lowers FLOPs by $50\times$ and memory by $32\times$, reducing the footprint from 45.09 MB to just 1.41 MB. Importantly, competing methods such as FedBAT and FedMUD do not provide any meaningful reduction in FLOPs or memory usage during runtime, as they retain full-precision computation despite performing efficient communication. These efficiency gains make FedBNN uniquely suitable for deployment in resource-constrained federated environments.

4.3.3 Post-training binarization performance comparison

When evaluated under equal FLOPs and memory budgets, i.e., after post-training binarization, FedBNN dramatically outperforms all competing approaches. In our evaluation, post-training binarization is performed by applying a sign function to the weights and activations with layer-wise norm scaling, i.e., $\mathbf{w}_b = \frac{|\mathbf{w}|\text{sign}(\mathbf{w})}{|\mathbf{w}_b|}$, where α is computed from the weight norm to preserve magnitude information. Because binarization is integrated throughout training, FedBNN exhibits negligible performance degradation between clean and binarized evaluation. On FMNIST, FedBNN maintains 88.46%, 87.76%, and 83.38% binarized accuracy, whereas FedAvg degrades to 53.42%, 63.68%, and 54.72%, and FedBAT collapses to single-digit accuracy. On SVHN and CIFAR10, similar trends are observed: FedBNN’s binarized accuracy remains close to its clean accuracy, while FedAvg, FedBAT, and FedMUD experience severe drops. This contrast becomes extreme on Tiny-ImageNet, and FEMNIST, where FedAvg falls to approximately 1–2% binarized accuracy, whereas FedBNN retains 60.04%, 46.54%, and $\sim 80\%$, respectively. Even for ConvNeXt-Tiny on CIFAR10, FedBNN’s binarized accuracy exactly matches its clean performance, confirming its robustness across modern architectures. Overall, although FedBNN incurs a modest clean-accuracy gap relative to FedAvg, its com-

binarization of massive efficiency gains and unmatched robustness to binarization makes it the most practical and deployment-ready method among all evaluated baselines.

Table 2: Ablation study for $N_c = 100$ comparing with and without server aggregation.

Method	Dataset (Model)	IID	Non-IID 1	Non-IID 2
FedBNN	FMNIST	88.46	87.76	83.38
FedBNN ($\beta = 1, \lambda = 1$)	(CNN4)	88.54	87.68	82.48
FedBNN	SVHN	86.89	85.63	84.40
FedBNN ($\beta = 1, \lambda = 1$)	(CNN4)	86.77	85.38	84.13
FedBNN	CIFAR10	89.95	82.84	73.82
FedBNN ($\beta = 1, \lambda = 1$)	(ResNet10)	89.34	82.82	68.54
FedBNN	Tiny-ImageNet	46.54	43.00	45.74
FedBNN ($\beta = 1, \lambda = 1$)	(ResNet18)	42.86	40.62	43.90
FedBNN	FEMNIST	79.73	80.31	79.13
FedBNN ($\beta = 1, \lambda = 1$)	(ResNet18)	79.10	79.61	80.68

4.3.4 Ablation Study: Importance of server alignment

To evaluate the role of server-side alignment, we perform an ablation by setting $\beta = 1$ in Eq. (14), which removes the influence of the previous global model \mathbf{w}_t . The update rule then becomes

$$\tilde{\mathbf{w}} = \mathbf{w}_{t+1} + \alpha (\mathbf{w}_{R,t+1} - \mathbf{w}_{t+1}), \quad (26)$$

effectively disabling the alignment term that stabilizes the global update across communication rounds. Also, λ_l is set to 1 to remove the influence of the server during rotation optimization. Table 2 shows that incorporating server alignment consistently improves performance across most datasets and splits. The largest gains appear under heterogeneous settings. For example, on CIFAR10 (ResNet10) with Non-IID 2, accuracy increases from 68.54% to 73.82% (+5.28%). Similarly, on Tiny-ImageNet (ResNet18), IID accuracy improves from 42.86% to 46.54%, with additional gains under Non-IID 1 (2.38%). Smaller but consistent improvements are also observed on FMNIST and SVHN. These results highlight that server-side alignment helps maintain global consistency when aggregating rotated weights, leading to more stable binarized models and improved performance, particularly under heterogeneous data distributions. We further explored direct aggregation of $\tilde{\mathbf{w}}$ from each client in comparison to aggregating $\mathbf{R}_k^\top \mathbf{w}_k$. The results are discussed in the appendix.

5 Conclusion

We proposed FedBNN, a rotation-aware Binary Neural Network framework for federated learning that achieves accuracies within 10% of real-valued models while reducing runtime FLOPs by up to $58\times$ and memory by $32\times$. FedBNN also surpasses baselines such as FedBAT in some Non-IID cases and delivers superior post-training binarized accuracy, highlighting the benefits of including binarization during training. FedBNN strikes a strong balance between accuracy and efficiency, making it well-suited for scalable, lightweight federated learning. Future work will explore alternative aggregation strategies and larger architectures.

References

- Michael Crawshaw and Mingrui Liu. Federated learning under periodic client participation and heterogeneous data: A new communication-efficient algorithm and analysis. *Advances in Neural Information Processing Systems*, 37:8240–8299, 2024.
- Zhishuai Guo and Tianbao Yang. Communication-efficient federated group distributionally robust optimization. *Advances in Neural Information Processing Systems*, 37:23040–23077, 2024.
- Tzu-Ming Harry Hsu, Hang Qi, and Matthew Brown. Measuring the effects of non-identical data distribution for federated visual classification. *arXiv preprint arXiv:1909.06335*, 2019.
- Sixu Hu, Linshan Jiang, and Bingsheng He. Practical hybrid gradient compression for federated learning systems. In *Proceedings of the Thirty-Third International Joint Conference on Artificial Intelligence, Jeju, Republic of Korea*, pp. 3–9, 2024.
- Itay Hubara, Matthieu Courbariaux, Daniel Soudry, Ran El-Yaniv, and Yoshua Bengio. Binarized neural networks. *Advances in neural information processing systems*, 29, 2016.
- Geeho Kim, Jinkyu Kim, and Bohyung Han. Communication-efficient federated learning with accelerated client gradient. In *Proceedings of the IEEE/CVF Conference on Computer Vision and Pattern Recognition*, pp. 12385–12394, 2024a.
- Minsu Kim, Walid Saad, Merouane Debbah, and Choong S Hong. Spaff: Communication-efficient federated learning with sparse models and low computational overhead. *Advances in Neural Information Processing Systems*, 37:86500–86527, 2024b.
- Sangmin Lee and Hyeryung Jang. Bipruneff: Computation and communication efficient federated learning with binary quantization and pruning. *IEEE Access*, 13:42441–42456, 2025. doi: 10.1109/ACCESS.2025.3547627.
- Shiwei Li, Wenchao Xu, Haozhao Wang, Xing Tang, Yining Qi, Shijie Xu, Weihong Luo, Yuhua Li, Xiuqiang He, and Ruixuan Li. Fedbat: communication-efficient federated learning via learnable binarization. *arXiv preprint arXiv:2408.03215*, 2024.
- Shiwei Li, Xiandi Luo, Haozhao Wang, Xing Tang, Shijie Xu, Weihong Luo, Yuhua Li, Xiuqiang He, and Ruixuan Li. The panaceas for improving low-rank decomposition in communication-efficient federated learning. *arXiv preprint arXiv:2505.23176*, 2025.
- Tian Li, Anit Kumar Sahu, Manzil Zaheer, Maziar Sanjabi, Ameet Talwalkar, and Virginia Smith. Federated optimization in heterogeneous networks. *Proceedings of Machine learning and systems*, 2:429–450, 2020.
- Mingbao Lin, Rongrong Ji, Zihan Xu, Baochang Zhang, Yan Wang, Yongjian Wu, Feiyue Huang, and Chia-Wen Lin. Rotated binary neural network. *Advances in Neural Information Processing Systems*, 33, 2020.
- Xiang Liu, Liangxi Liu, Feiyang Ye, Yunheng Shen, Xia Li, Linshan Jiang, and Jialin Li. Fedlpa: One-shot federated learning with layer-wise posterior aggregation. *Advances in Neural Information Processing Systems*, 37:81510–81548, 2024.
- Xinyi Lu, Hao Zhang, Chenglin Li, Weijia Lu, Zhifei Yang, Wenrui Dai, Xiaofeng Ma, Can Zhang, Junni Zou, Hongkai Xiong, et al. Fedsmu: Communication-efficient and generalization-enhanced federated learning through symbolic model updates. *International Conference on Machine Learning*, 2025.
- Brendan McMahan, Eider Moore, Daniel Ramage, Seth Hampson, and Blaise Aguera y Arcas. Communication-efficient learning of deep networks from decentralized data. In *Artificial intelligence and statistics*, pp. 1273–1282. PMLR, 2017.
- Mohammad Rastegari, Vicente Ordonez, Joseph Redmon, and Ali Farhadi. Xnor-net: Imagenet classification using binary convolutional neural networks. In *European conference on computer vision*, pp. 525–542. Springer, 2016.

Suhail Mohmad Shah and Vincent K. N. Lau. Model compression for communication efficient federated learning. *IEEE Transactions on Neural Networks and Learning Systems*, 34(9):5937–5951, 2023. doi: 10.1109/TNNLS.2021.3131614.

Nitin Priyadarshini Shankar, Deepsayan Sadhukhan, Nancy Nayak, Thulasi Tholeti, and Sheetal Kalyani. Binarized resnet: Enabling robust automatic modulation classification at the resource-constrained edge. *IEEE Transactions on Cognitive Communications and Networking*, 10(5):1913–1927, 2024. doi: 10.1109/TCCN.2024.3391325.

Yuzhi Yang, Zhaoyang Zhang, and Qianqian Yang. Communication-efficient federated learning with binary neural networks. *IEEE Journal on Selected Areas in Communications*, 39(12):3836–3850, 2021.

A Appendix

A.1 Aggregating $\tilde{\mathbf{w}}$

In this section, we describe an alternative server-side aggregation formulation for model evaluation. Instead of first aggregating rotation-aligned weights and then forming the global model, the server constructs the adjustable rotated weight vector ($\tilde{\mathbf{w}}_k$) for each client and subsequently aggregates them. After local training, each client k sends its updated real-valued weights \mathbf{w}_k together with the learned rotation matrices \mathbf{R}_k to the server. Rather than aggregating the client weights beforehand, the server directly computes $\tilde{\mathbf{w}}_k$ for each client using the local weights and their corresponding rotation-aligned representations.

$$\tilde{\mathbf{w}}_k = \mathbf{w}_k + \alpha\beta (\mathbf{R}_k^\top \mathbf{w}_k - \mathbf{w}_k) + \alpha(1 - \beta) (\mathbf{w}_t - \mathbf{w}_k). \quad (27)$$

Each $\tilde{\mathbf{w}}_k$ incorporates the client-specific rotation-aligned weights while preserving the influence of the client’s local update. These auxiliary models are then aggregated using the same weighting factors as in FedAvg:

$$\tilde{\mathbf{w}} = \sum_{k=1}^{N_k} \frac{N_{sk}}{N_s} \tilde{\mathbf{w}}_k. \quad (28)$$

The aggregated auxiliary model $\tilde{\mathbf{w}}$ is used only for server-side evaluation and model selection and is never transmitted to clients. The model broadcast to clients for the next communication round remains the standard FedAvg model obtained by aggregating the real-valued weights.

Table 3: Ablation study under different aggregation and binarization strategies for $N_c = 100$.

Method	Dataset (Model)	Accuracy		
		IID	Non-IID 1	Non-IID 2
FedBNN	FMNIST	88.46	87.76	83.38
Aggregating $\tilde{\mathbf{w}}$	(CNN4)	87.88	87.24	80.40
FedBNN	SVHN	86.89	85.63	84.40
Aggregating $\tilde{\mathbf{w}}$	(CNN4)	86.25	84.74	80.40
FedBNN	CIFAR10	89.95	82.84	73.82
Aggregating $\tilde{\mathbf{w}}$	(ResNet10)	89.82	82.22	55.62
FedBNN	Tiny-ImageNet	46.54	43.00	45.74
Aggregating $\tilde{\mathbf{w}}$	(ResNet18)	46.36	42.46	43.84
FedBNN	FEMNIST	79.73	80.31	79.13
Aggregating $\tilde{\mathbf{w}}$	(ResNet18)	80.56	80.76	76.41
FedBNN	CIFAR10	72.08	67.08	63.00
Aggregating $\tilde{\mathbf{w}}$	(ConvNeXt-Tiny)	72.62	66.60	62.70

Table 3 summarizes the performance across multiple datasets, models, and data heterogeneity settings. Overall, aggregating the rotation-aligned weights prior to forming the auxiliary update consistently provides better or more stable performance. For FMNIST with CNN4, the proposed method achieves higher accuracy under all data distributions, obtaining 88.46%, 87.76%, and 83.38% for IID, Non-IID 1, and Non-IID 2 settings, respectively, compared to 87.88%, 87.24%, and 80.40% for the alternative aggregation. Similarly, on SVHN with CNN4, FedBNN improves accuracy across all settings, reaching 86.89%, 85.63%, and 84.40%, outperforming the alternative approach which achieves 86.25%, 84.74%, and 80.40%.

The benefits are particularly pronounced on more challenging datasets. For CIFAR10 with ResNet10 under the most heterogeneous Non-IID 2 setting, the proposed aggregation achieves 73.82% accuracy, compared to only 55.62% with $\tilde{\mathbf{w}}_k$, indicating significantly improved robustness to client heterogeneity. On Tiny-ImageNet with ResNet18, the proposed method also provides consistent gains, achieving 46.54%, 43.00%, and 45.74% across the three distributions, compared to 46.36%, 42.46%, and 43.84% for the alternative strategy.

A similar trend is observed on the FEMNIST dataset with ResNet18, where the proposed aggregation achieves competitive or superior performance, particularly under Non-IID conditions. Finally, for CIFAR10 with ResNet18, the differences are small under IID settings but remain comparable under heterogeneous data distributions. These results indicate that performing aggregation in the rotation-aligned space before constructing the auxiliary update better preserves the binarization structure across clients. In contrast, aggregating the auxiliary models $\tilde{\mathbf{w}}_k$ introduces additional averaging after the nonlinear alignment step, potentially diluting the alignment benefits. Consequently, the proposed FedBNN aggregation strategy yields more stable and often higher accuracy across datasets and heterogeneity settings.

We observe a slight performance drop for FedBNN in the IID setting on FEMNIST and CIFAR10 (ResNet18) compared to directly aggregating $\tilde{\mathbf{w}}$. This behavior can be attributed to the interaction between binary constraints and homogeneous client updates. Under IID data distributions, client gradients are highly aligned, and aggregating real-valued weights $\tilde{\mathbf{w}}$ allows the server to average updates in the continuous parameter space with minimal information loss. In contrast, FedBNN aggregates in the binarized weight space, introducing a small quantization error due to the sign operation. While this discretization acts as a useful regularizer under heterogeneous data distributions, in the IID case, it can slightly limit the expressiveness of the aggregated model, particularly for deeper architectures such as ResNet18 used in FEMNIST and CIFAR10. Consequently, the real-valued aggregation occasionally yields marginally higher accuracy in IID settings, whereas FedBNN provides greater robustness as data heterogeneity increases.

A.2 Ablation Study: Importance of server alignment, additional results

For the ConvNext-Tiny architecture considered in Section 4.3.4, Table 4 further highlights the importance of server alignment. The full FedBNN framework achieves 72.08%, 67.08%, and 63.00% accuracy under IID, Non-IID 1, and Non-IID 2 settings, respectively. When server alignment is removed by setting $\beta = 1$ and $\lambda = 1$, the performance drops to 70.78%, 61.78%, and 58.50%. The larger degradation under Non-IID distributions indicates that server alignment is particularly important for maintaining consistency across heterogeneous clients.

Table 4: Ablation study for $N_c = 100$ comparing with and without server aggregation.

Method	Dataset (Model)	Accuracy		
		IID	Non-IID 1	Non-IID 2
FedBNN	CIFAR10	72.08	67.08	63.00
FedBNN ($\beta = 1, \lambda = 1$)	(ConvNext-Tiny)	70.78	61.78	58.50

A.3 Comparison with Real-Valued Networks of Similar Complexity

Table 5 compares FedBNN with real-valued ResNet models whose architecture is reduced such that both the training and inference complexity approximately match the FLOPs and memory footprint of FedBNN at inference. This differs from the experiment presented in Section 4.3.3 of the main paper, where full-sized real-valued models are trained, and only the inference complexity is reduced through post-training binarization.

When the real-valued networks are scaled down to match the computational and memory constraints of FedBNN, their performance drops significantly. On CIFAR10, FedBNN with ResNet10 achieves 73.82% accuracy in the most challenging Non-IID 2 setting, outperforming the FLOPs-matched and memory-matched real-valued models by 7.66% and 5.04%, respectively. Similar trends are observed for IID and Non-IID 1 settings, where FedBNN maintains competitive or superior accuracy while operating at comparable computational and memory budgets.

A similar pattern is observed on TinyImageNet with ResNet18. Under Non-IID 2, FedBNN achieves 45.74% accuracy, which is substantially higher than the FLOPs-matched and memory-matched real-valued models that achieve 35.66% and 39.24%, respectively. Even under IID and moderately non-IID settings, FedBNN consistently performs better when the model complexity is constrained.

Table 5: Performance comparison for $N_c = 100$. The FLOPs and memory values are calculated during runtime.

Method	Dataset	(Model)	Accuracy			FLOPs	Memory (MB)
			IID	Non-IID 1	Non-IID 2		
FedBNN	CIFAR10	ResNet10	89.95	82.84	73.82	1.11×10^7	0.61
FedAvg		ResNet10	90.86	86.28	70.62	4.40×10^8	19.62
FedAvg		ResNet10	84.74	81.06	66.16	1.12×10^7	0.49
FedAvg		(FLOPs matched)	ResNet10	86.60	81.50	68.78	1.35×10^7
FedBNN	TinyImageNet	ResNet18	46.54	43.00	45.74	9.05×10^7	1.41
FedAvg		ResNet18	55.00	52.62	54.54	4.44×10^8	45.09
FedAvg		ResNet18	41.06	37.72	35.66	8.99×10^7	0.95
FedAvg		(FLOPs matched)	ResNet18	43.16	40.54	39.24	1.33×10^8
FedAvg	(Memory matched)	ResNet18					

These results highlight that when the entire model capacity must be reduced to satisfy strict computational and memory limits, training directly with binarized networks is significantly more effective than shrinking real-valued architectures to the same complexity. Combined with the results in Section X that study post-training binarization, this analysis demonstrates that FedBNN provides strong performance across both practical deployment scenarios.

A.4 Communication overhead for transmitting \mathbf{R}_1 and \mathbf{R}_2 from client to the server

Table 6: Parameter overhead of the rotation matrices \mathbf{R}_1 and \mathbf{R}_2 in FedBNN. Across all datasets and architectures, the additional parameters remain below 1% of the model weights, demonstrating negligible overhead (in comparison to FedAvg) and good scalability to larger models.

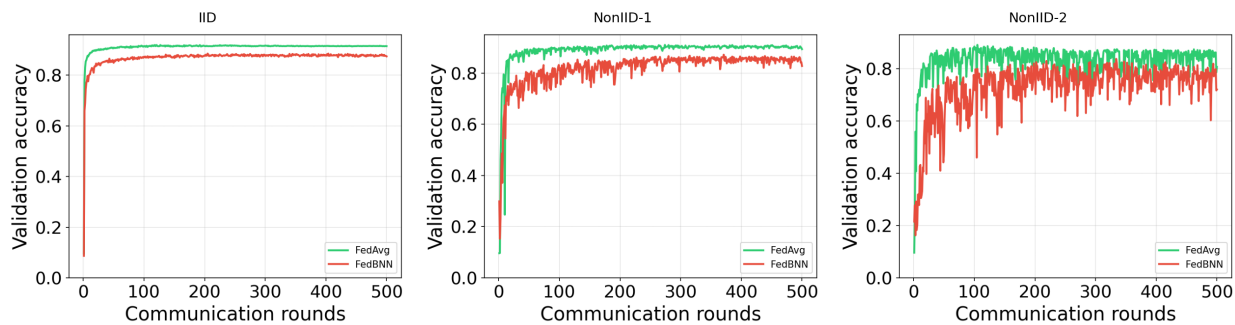
Method	Dataset	Model	No of parameters for \mathbf{w}	No of parameters for $\mathbf{R}_1, \mathbf{R}_2$	Overhead Percentage
FedBNN	FMNIST	CNN4	387,360	4,070	1.05%
	SVHN	CNN4	387,936	4,142	1.07%
	CIFAR10	ResNet10	4,890,624	27,552	0.56%
	FEMNIST	ResNet18	11,157,504	62,272	0.56%
	TinyImageNet	ResNet18	11,157,504	62,272	0.56%
	CIFAR10	ConvNext-Tiny	27,751,392	78,084	0.28%

Table 6 reports the parameter overhead introduced by the rotation matrices \mathbf{R}_1 and \mathbf{R}_2 used in FedBNN across different datasets and model architectures. The results show that the additional parameters required for the rotation matrices are negligible compared to the total number of weight parameters \mathbf{w} . For smaller models, such as CNN4 on FMNIST and SVHN, the overhead is approximately 1%, whereas for larger architectures, such as ResNet10 and ResNet18, the overhead drops to around 0.56%. For even larger models such as ConvNext-Tiny, the overhead further decreases to only 0.28%. This trend occurs because the number of rotation parameters grows much more slowly than the total number of model weights. Overall, the results demonstrate that FedBNN introduces minimal parameter overhead (compared to FedAvg) while enabling

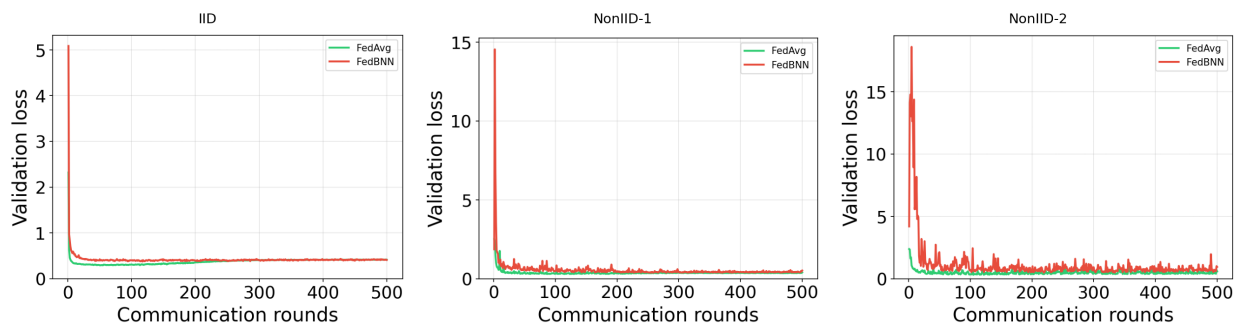
rotation-based alignment, making the method scalable to larger architectures without significantly increasing model size or communication cost.

A.5 Convergence of FedBNN vs FedAvg

We compare the validation accuracy and validation loss of FedBNN against FedAvg across multiple datasets (FMNIST, SVHN, CIFAR-10, FEMNIST, Tiny-ImageNet), architectures (CNN-4, ResNet-10, ConvNeXt-Tiny, ResNet-18), and data-heterogeneity settings (IID, NonIID-1, and NonIID-2). The validation accuracy and validation loss curves (see Figures 2, 3, 4, 5, 6, 7) show that FedBNN consistently achieves competitive or superior performance relative to FedAvg. Under IID data, FedBNN closely tracks or matches FedAvg while operating with binary weights and rotation-based aggregation, demonstrating that the rotation mechanism preserves useful representations. Under non-IID partitions, FedBNN often achieves higher validation accuracy and lower validation loss than FedAvg, with the gap widening as heterogeneity increases. This suggests that the client-specific rotations in FedBNN provide an effective inductive bias for heterogeneous federated learning, mitigating the negative effects of data skew that typically hinder FedAvg. Overall, these results indicate that FedBNN is a promising approach for federated learning with binary neural networks, offering a favorable accuracy–efficiency trade-off without sacrificing (and at times improving) generalization compared to full-precision FedAvg.

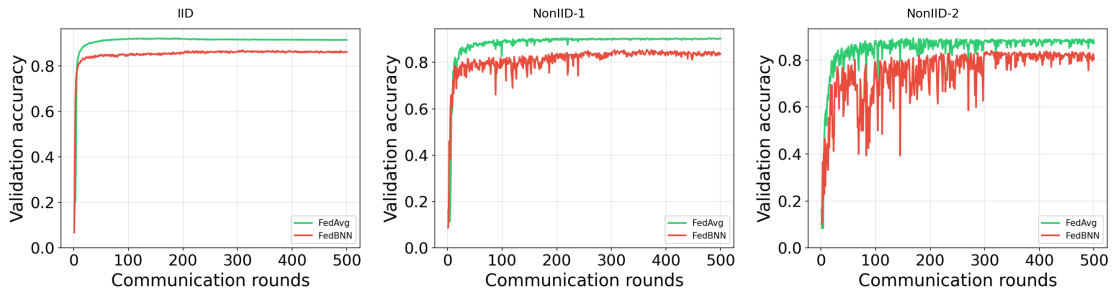


(a) FMNIST CNN4 — Validation Accuracy

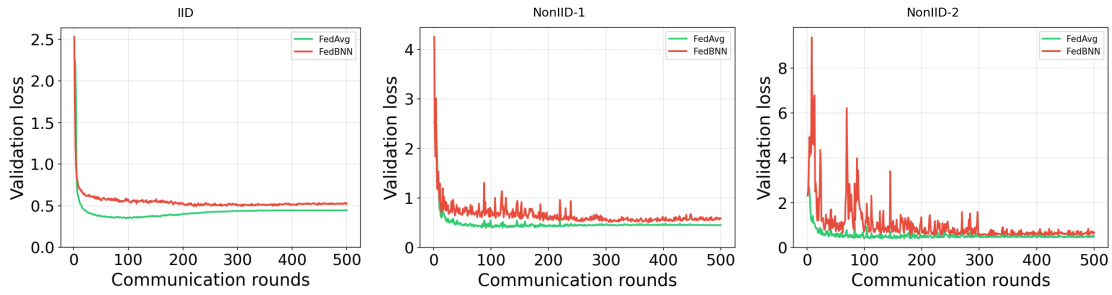


(b) FMNIST CNN4 — Validation Loss

Figure 2: Performance comparison between FedAvg and FedBNN on FMNIST using the CNN4 architecture under IID, Non-IID1 (Dirichlet $\alpha = 0.3$), and Non-IID2 (label-skew) data partitions.

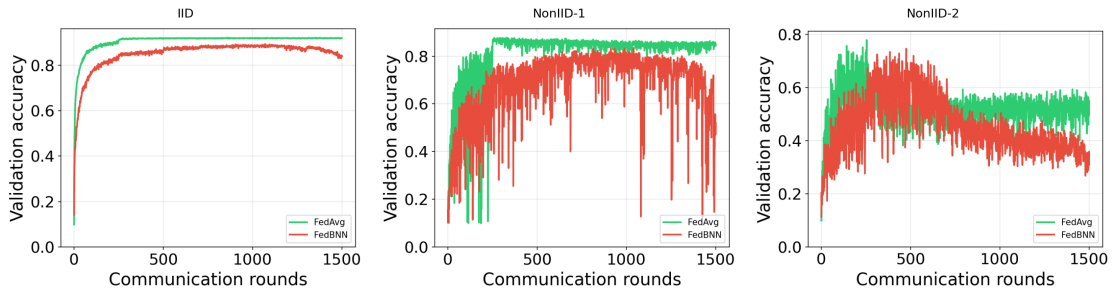


(a) SVHN CNN4 — Validation Accuracy

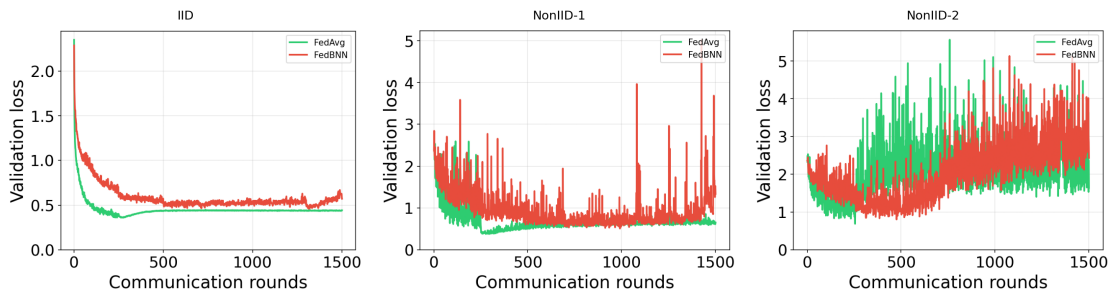


(b) SVHN CNN4 — Validation Loss

Figure 3: Performance comparison between FedAvg and FedBNN on SVHN using the CNN4 architecture under IID, Non-IID1 (Dirichlet $\alpha = 0.3$), and Non-IID2 (label-skew) data partitions.

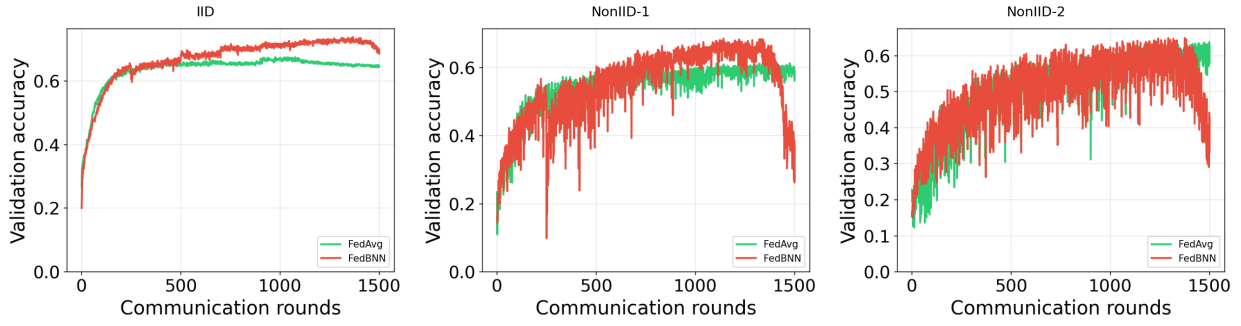


(a) CIFAR10 ResNet10 — Validation Accuracy

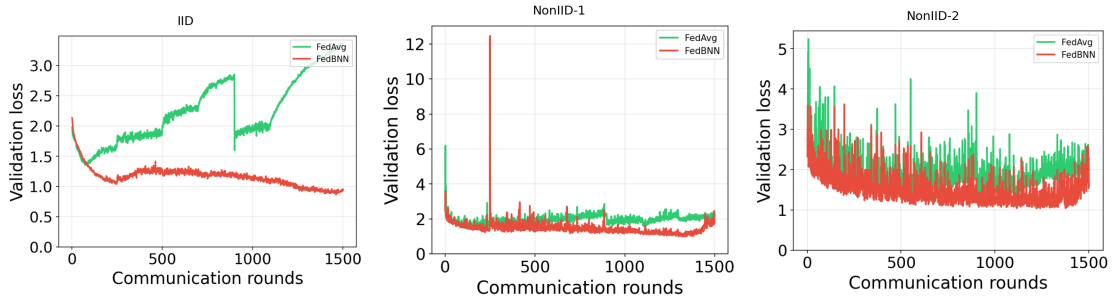


(b) CIFAR10 ResNet10 — Validation Loss

Figure 4: Performance comparison between FedAvg and FedBNN on CIFAR10 using the ResNet10 architecture under IID, Non-IID1 (Dirichlet $\alpha = 0.3$), and Non-IID2 (label-skew) data partitions.

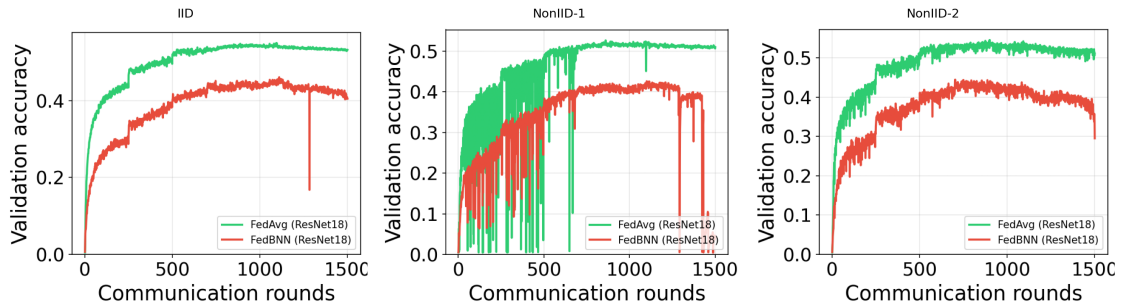


(a) CIFAR10 ConvNeXt-Tiny — Validation Accuracy

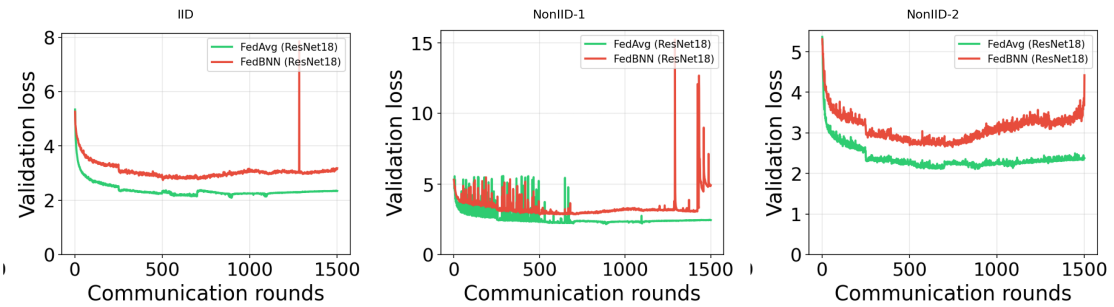


(b) CIFAR10 ConvNeXt-Tiny — Validation Loss

Figure 5: Performance comparison between FedAvg and FedBNN on CIFAR10 using the ConvNeXt-Tiny architecture under IID, Non-IID1 (Dirichlet $\alpha = 0.3$), and Non-IID2 (label-skew) data partitions.

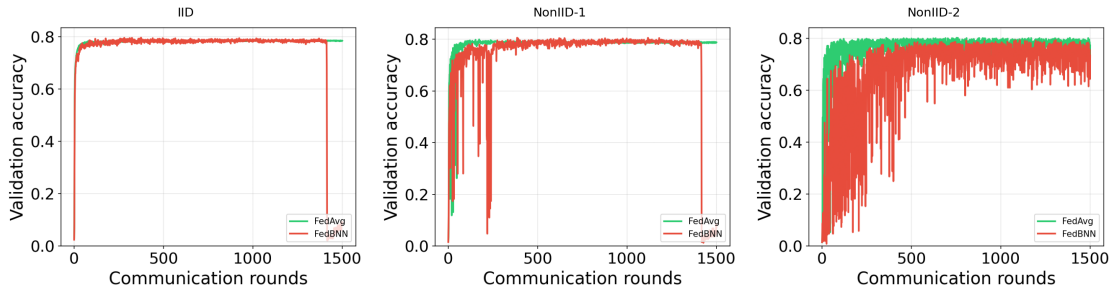


(a) TinyImageNet ResNet18 — Validation Accuracy

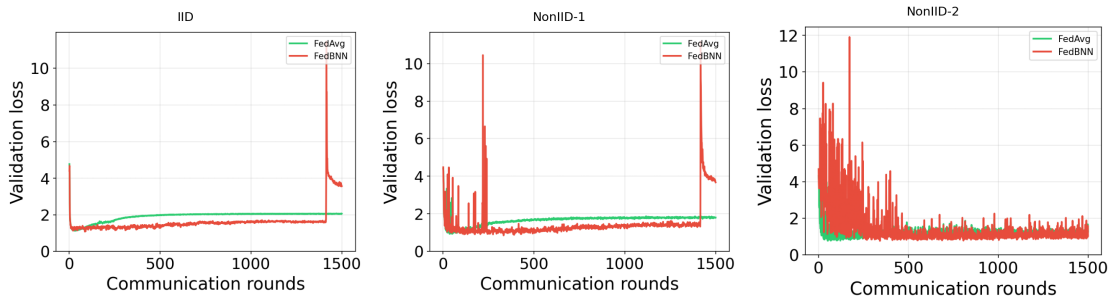


(b) TinyImageNet ResNet18 — Validation Loss

Figure 6: Performance comparison between FedAvg and FedBNN on TinyImageNet using the ResNet18 architecture under IID, Non-IID1 (Dirichlet $\alpha = 0.3$), and Non-IID2 (label-skew) data partitions.



(a) FEMNIST ResNet18 — Validation Accuracy



(b) FEMNIST ResNet18 — Validation Loss

Figure 7: Performance comparison between FedAvg and FedBNN on FEMNIST using the ResNet18 architecture under IID, Non-IID1 (Dirichlet $\alpha = 0.3$), and Non-IID2 (label-skew) data partitions.

A.6 Alpha, beta, lambda

We analyze the evolution of FedBNN’s aggregation parameters: λ , α , and β , over communication rounds and across layers, for multiple datasets (CIFAR-10, FEMNIST, Tiny-ImageNet) and data-heterogeneity settings (IID, NonIID-1 and NonIID-2). The plots in Figure 8, 9, 10, 11, 12 and 13 show, per round and per layer, four quantities: λ (server contribution before rotation optimization), $1 - \alpha$ (client weight contribution), $\alpha\beta$ (rotated weight contribution), and $\alpha(1 - \beta)$ (server contribution). A vertical line marks the round at which the model attains its best validation accuracy. These visualizations reveal how the balance between server and client contributions, and between rotated and non-rotated terms, evolves during training; the round of best validation performance often coincides with a favorable regime of these quantities, supporting the role of the rotation mechanism in FedBNN’s convergence. The per-layer variation indicates that different layers adapt their client-versus-server and rotation weighting differently under federated training, which is consistent with the design of client-specific rotations that help align binary representations across non-IID clients. Overall, the α - β - λ analysis provides empirical evidence that FedBNN’s parameterization is well-behaved across datasets and heterogeneity levels and that the rotation-based aggregation is a key factor in its performance.

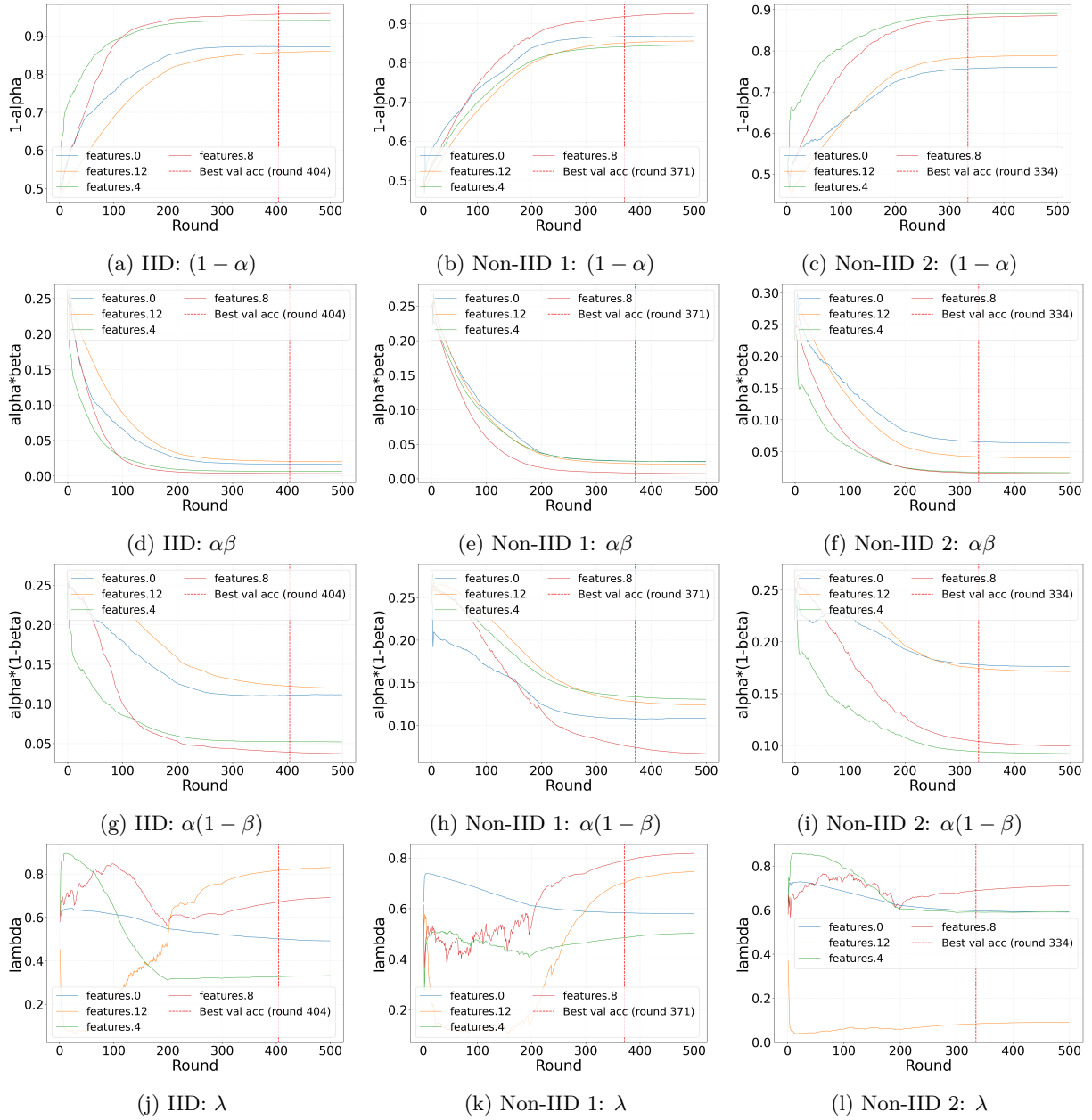


Figure 8: Hyperparameter sensitivity on FMNIST under IID, Non-IID1, and Non-IID2.

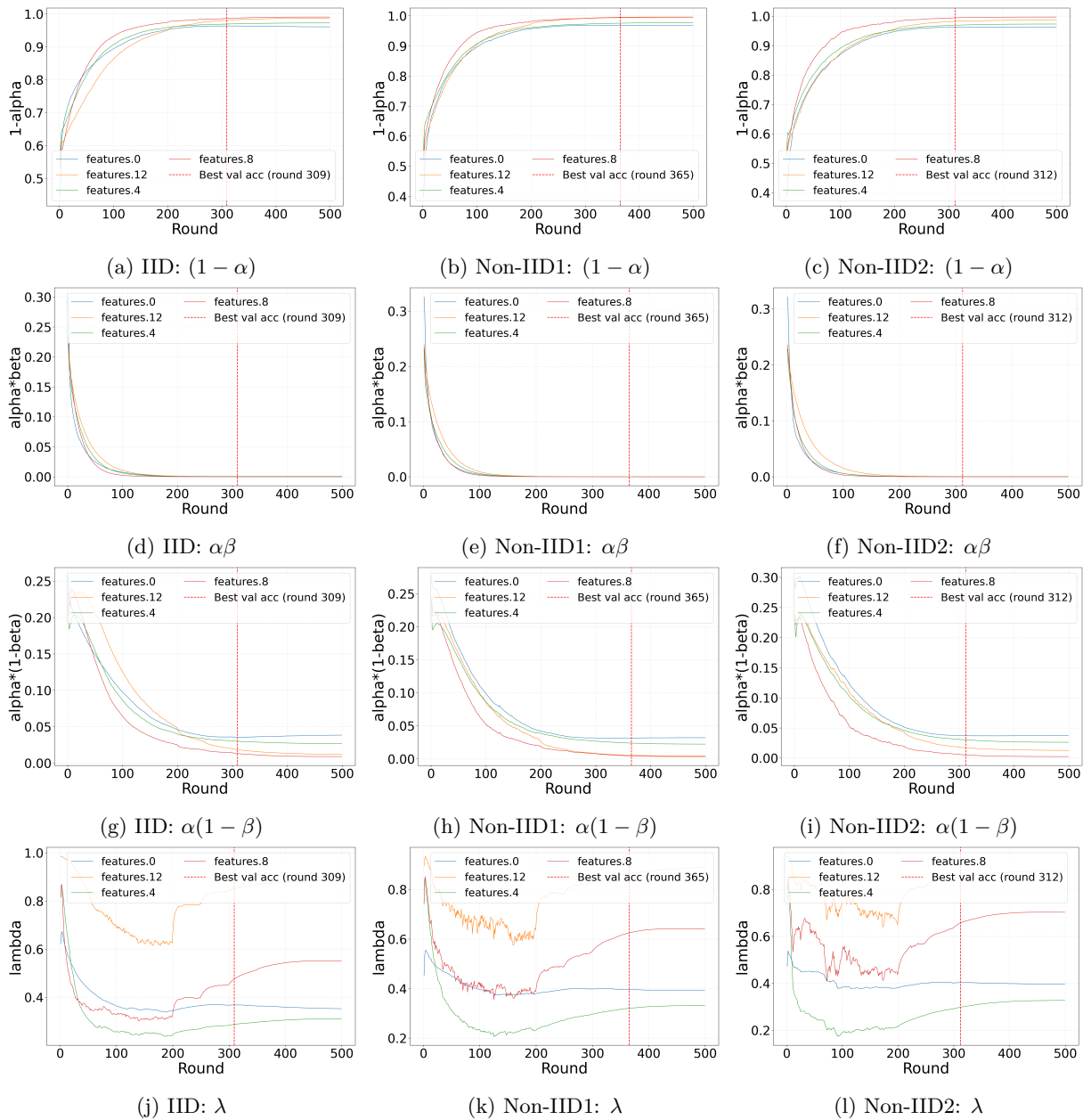


Figure 9: Hyperparameter sensitivity on SVHN under IID, Non-IID1, and Non-IID2.

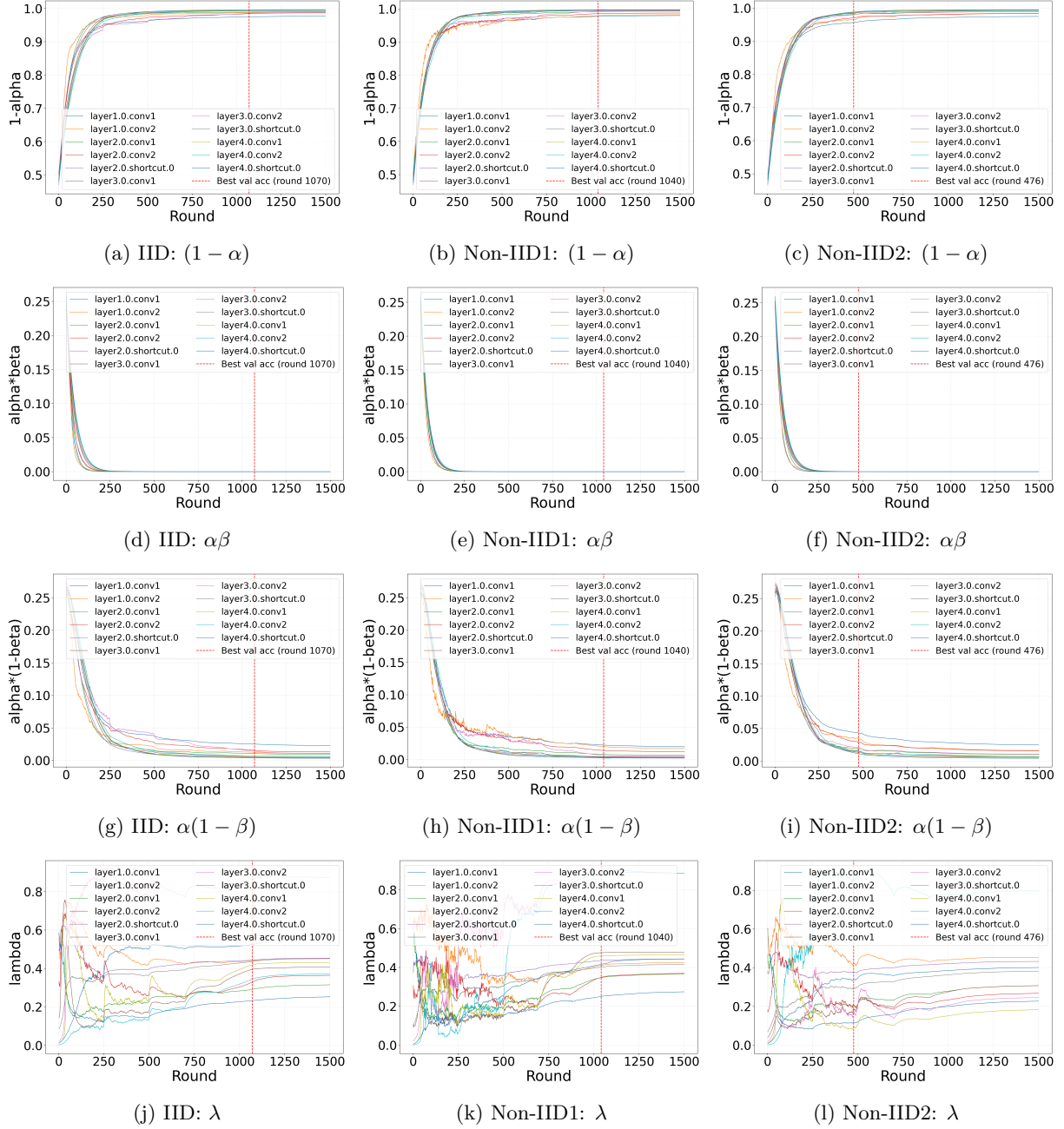


Figure 10: Hyperparameter sensitivity on CIFAR10 (ResNet10) under IID, Non-IID1, and Non-IID2 data heterogeneity settings.

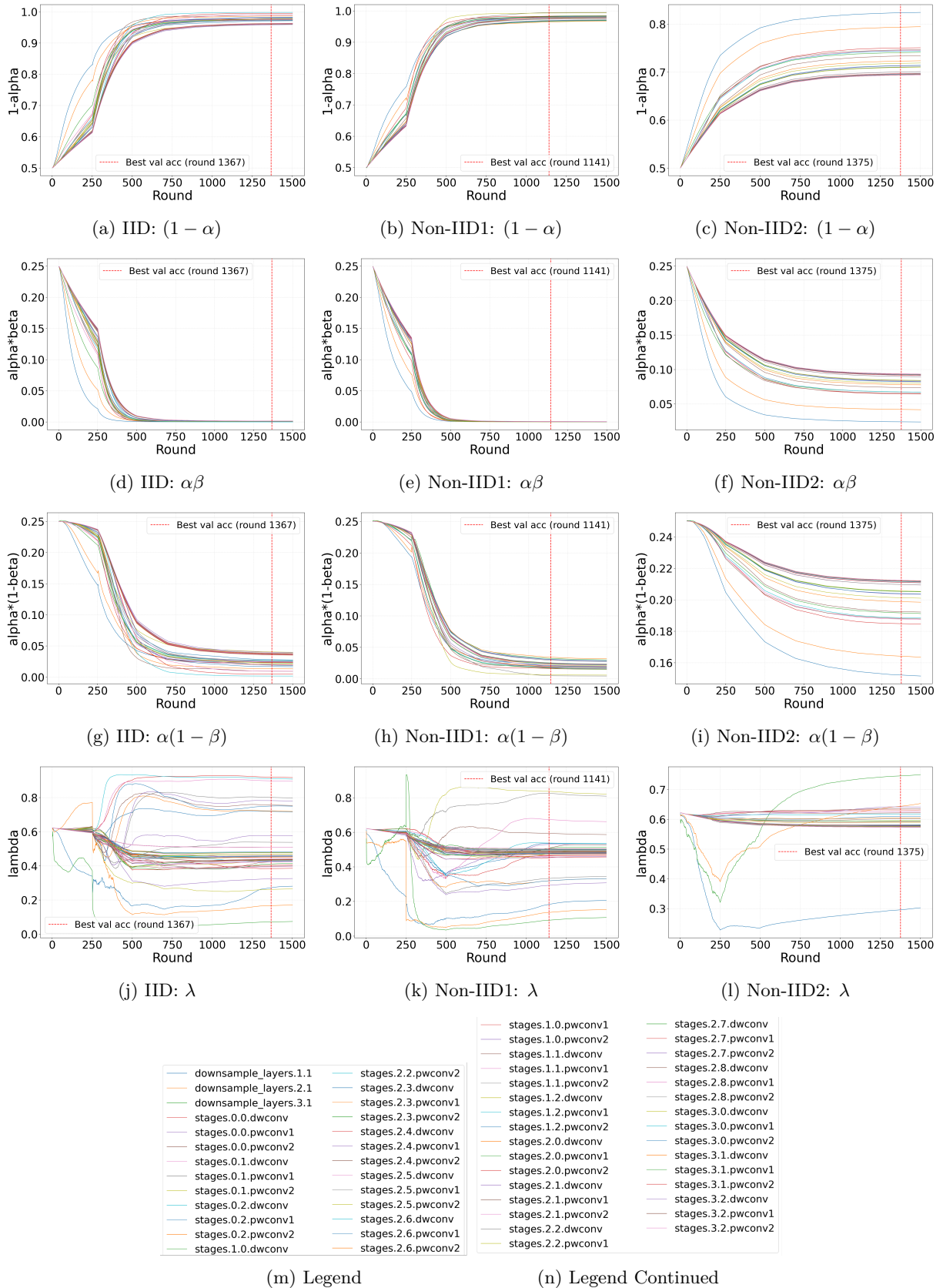


Figure 11: Sensitivity analysis of the hyperparameters $(1 - \alpha)$, $\alpha\beta$, $\alpha(1 - \beta)$, and λ on CIFAR10 (ConvNeXT-Tiny) under three data heterogeneity settings: IID, Non-IID1 (LabelCnt=0.3), and Non-IID2 (Dirichlet=0.3).

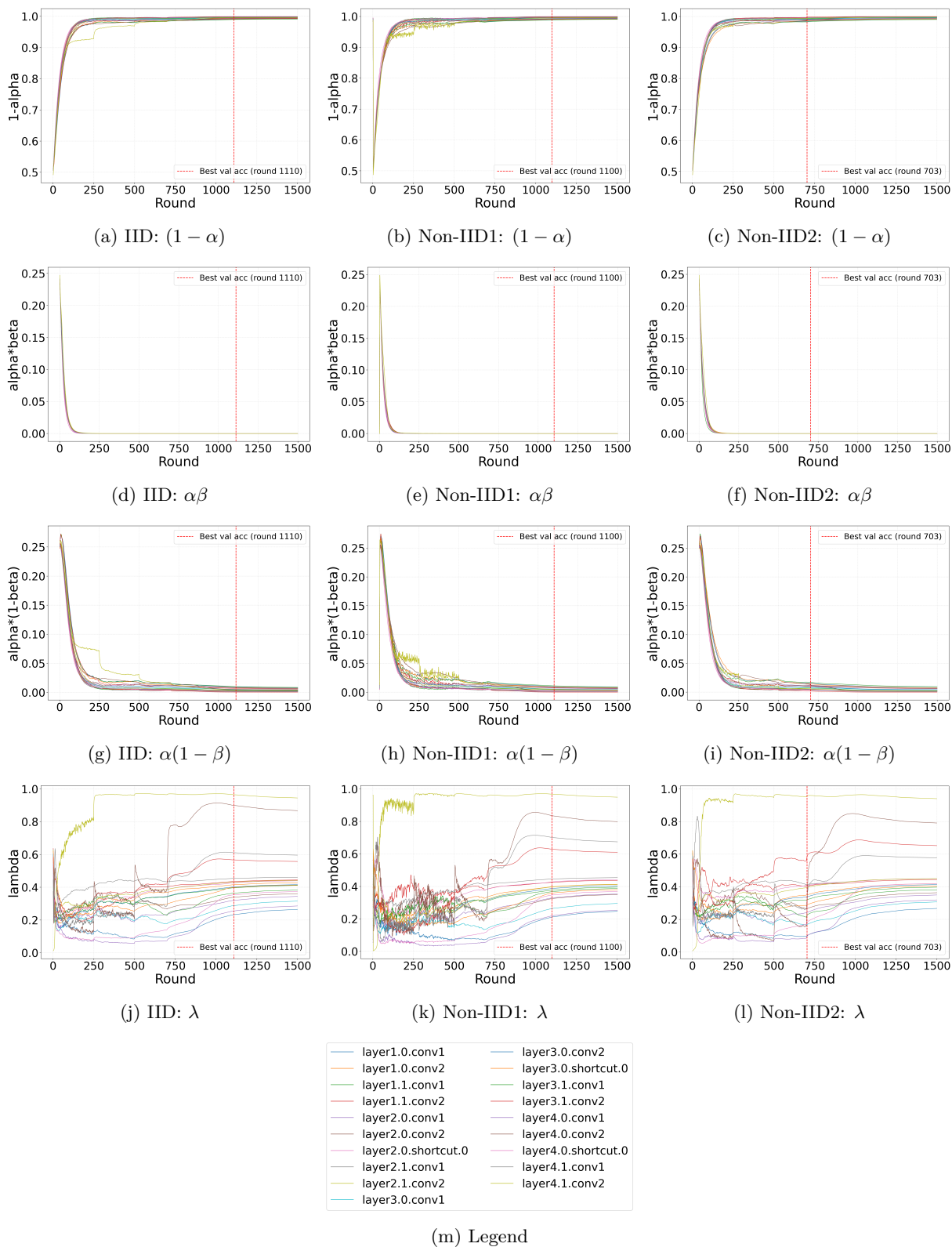


Figure 12: Hyperparameter sensitivity on TinyImageNet under IID, Non-IID1, and Non-IID2 settings.

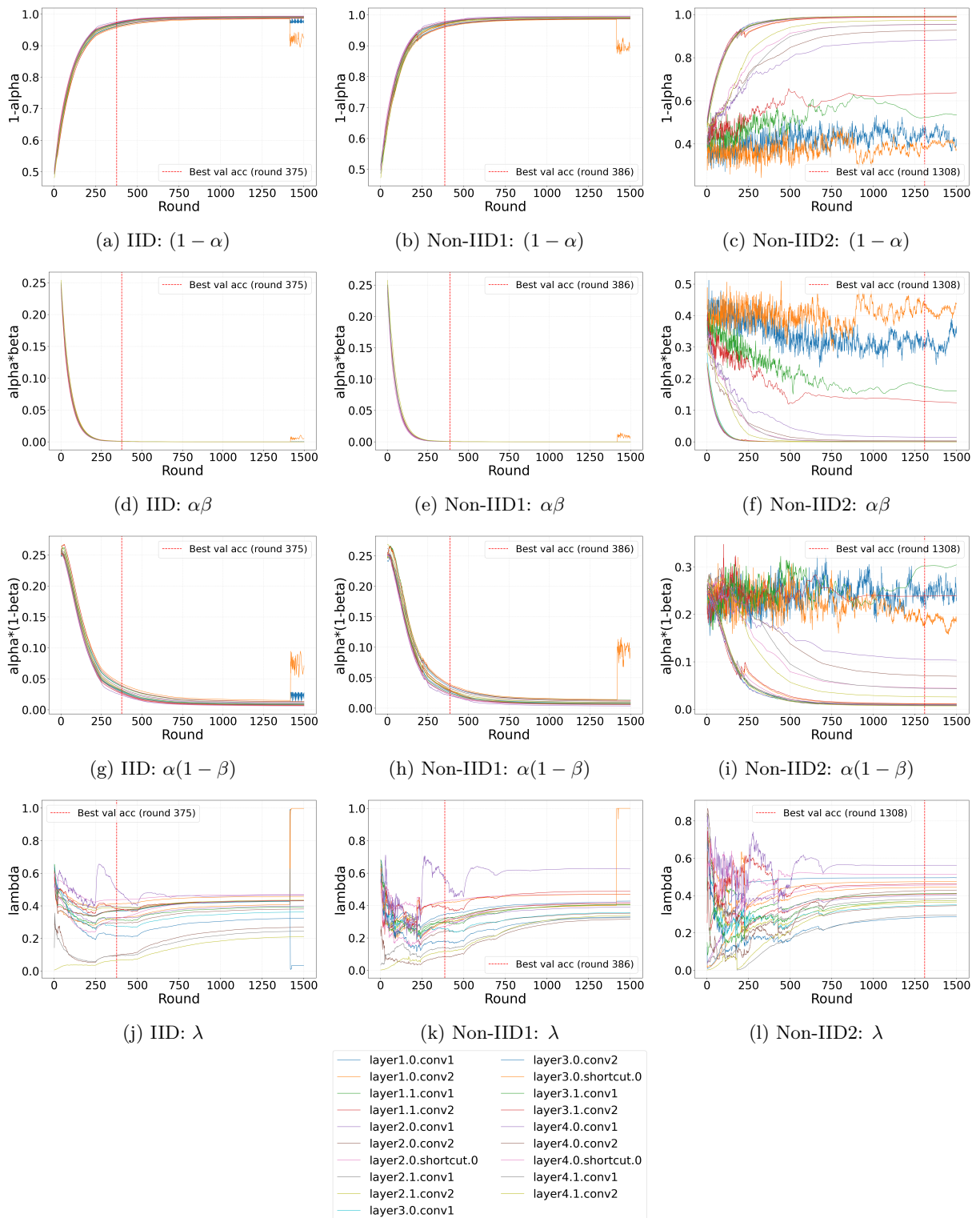


Figure 13: Hyperparameter sensitivity on FEMNIST under IID, Non-IID1, and Non-IID2 settings.